Communications in Physics, Vol. 24, No. 2 (2014), pp. 163-169

CHEMICAL COMPOSITION OF HIGH -T_C $Ge_{1-x}Mn_x$ NANOCOLUMNS GROWN ON GE(001) SUBSTRATES

LE THI GIANG AND NGUYEN MANH AN
Hong Duc University, 565 Quang Trung street, Thanh Hoa city, Vietnam

E-mail: lethigiang@hdu.edu.vn; nguyenmanhan@hdu.edu.vn

Received 04 April 2014
Accepted for publication 24 May 2014

Abstract. *By mean of molecular beam epitaxy (MBE) equipped with a reflexion high-energy electron diffraction (RHEED) technique, we have chosen an intermediate and appropriate substrate temperature of 130 $^\circ$C to reproducibly synthetize high-T_C $Ge_{1-x}Mn_x$ nanocolumns phase. Laser Pulse Atom Probe Tomography (LP-APT) technique have been used to determine at atomic scale the chemical composition inside nanocolumns and also in the surrounding diluted matrix. The Mn concentration inside nanocolumns is found to be highly inhomogeneous, it is about 20% at the bottom and can increase up to ∼40% in the top near the surface region. The Mn concentration in the matrix is about 0.25 % at the surface and can reach a highest value of ∼1% in regions close to the interface.*

Keywords: GeMn diluted magnetic semiconductors, chemical composition, high-T_C nanocolumns, thin film..

I. INTRODUCTION

Recently, ferromagnetic semiconductor which combines the advantages of semiconductor and magnetic material properties in a single semiconductor device has attracted a great interest. The research toward group IV-based magnetic semiconductor is stimulated by the theoretical prediction of a high Curie temperature based on the Zener model [1]. Among many group IV semiconductors, Ge has received much more attention due to its potential compatibility with current Si-based processing technology and higher intrinsic hole mobility than GaAs and Si. Following the first claim by Park *et al.* [2] that the Curie temperature of epitaxial Ge_{1-x} Mn_x increased (from 25 to 116 K) linearly with Mn concentration, several groups made great efforts on pursuing room-temperature ferromagnetism of Ge-based magnetic semiconductor by increasing Mn-doped concentration [3-12].

However, the use of $Ge_{1-x}Mn_x$ DMS has been, up to now, greatly hampered by its Curie temperature (T_C), which is well below room temperature. One of the difficulties to get high-T_C $Ge_{1-x}Mn_x$ alloys probably arises from a very low solubility of Mn in Ge matrix, which favors the formation of embedded precipitates and/or clusters inside the alloys, thus conducting to the formation of highly heterogeneous materials. Different kinds of embedded Mn-rich phases have been

identified, such as Mn-rich elongated structures [13], amorphous Mn-rich precipitates [14], self-assembled nanocolumns [12, 15] and the most commonly observed is probably metallic Mn_5Ge_3 clusters [16, 17]. For spintronic applications, the nanocolumn phase appears particularly interesting since it remains ferromagnetic up to temperatures above 400 K and exhibits semiconducting conductivity [12, 18, 19]. Nevertheless, the $Ge_{1-x}Mn_x$ nanocolumns grown in that condition are metastable, they transform into metallic Mn_5Ge_3 clusters upon post-growth thermal annealing at a temperature around 400 ° C. In order to stabilize this phase, it is crucial to investigate the composition and the mechanism leading to the formation of $Ge_{1-x}Mn_x$ nanocolumns. In [12], the composition of nanocolumns has been attributed to Ge_2Mn, a Ge-rich phase which does not exist in the bulk phase diagram [20].

Working on this direction, in this paper, we report on the results of analysing the chemical composition of high-T_C $Ge_{1-x}Mn_x$ nanocolumns grown on Ge(001) by MBE. Using LP-APT analyses, we are able to precisely determine at the atomic scale of the Mn concentration inside nanocolumns and in the diluted matrix.

II. EXPERIMENTAL SET-UP

$Ge_{1-x}Mn_x$ films were grown by molecular beam epitaxy (MBE) on epi-ready n-type Ge(001) wafers with a nominal resistivity of 10 Ω.cm at CINaM (Centre Interdisciplinaire de Nanosciences de Marseille, France). The base pressure in the MBE system is better than 5×10^{-10} Torr. The growth chamber is equipped with a reflexion high-energy electron diffraction (RHEED) technique to control the cleanness of the substrate surface prior to growth and to monitor the epitaxial growth process. $Ge_{1-x}Mn_x$ films were obtained by co-deposition of Ge and Mn from standard Knudsen effusion cells, the Ge deposition rate was determined from RHEED intensity oscillations whereas the Mn deposition rate was deduced from Rutherford backscattering spectrometry (RBS) measurements. For Mn concentrations below 2%, the measurement uncertainty can reach a value of 10%. The standard growth rate used in this work is of 1 – 2 nm/min.

The cleaning of Ge(001) substrate surfaces was carried out in two steps: a chemical cleaning to remove hydrocarbon related contaminants followed by an *in-situ* thermal cleaning at ∼750°C to remove the Ge surface oxide layers. After this step, the Ge(001) surface generally exhibits a (2×1) reconstruction. To insure a good starting Ge surface prior to $Ge_{1-x}Mn_x$ growth, a ∼30 nm thick Ge buffer layer was systematically grown at a substrate temperature of 600°C.

Structural analyses of the grown films were performed through extensive high resolution transmission electron microscopy (TEM) by using a JEOL 3010 microscope operating at 300 kV with a spatial resolution of 1.7 Å. Particularly, we have made in used the Laser Pulse Atom Probe Tomography (LP-APT) technique to determine at atomic scale the chemical composition inside nanocolumns and also in the surrounding diluted matrix. LP-APT measurements were performed using an Imago LEAP 3000X HR microscope in the pulsed laser mode. The analyses were carried out at 20.3 K, with a laser pulse frequency of 100 kH. The different samples were analyzed using a laser power of 0.1, 0.08 or 0.06 nJ, corresponding in our setup to a ratio I_{Ge}^{2+}/ I_{Ge}^{1+} of 3×10^1, 10^2, and 3×10^2, respectively.

III. RESULTS AND DISCUSSION

Since the first evidence in 2006 on the existence of a high-T_C nanocolumn phase by the CEA-Grenoble research group [12] and despite the interest that this phase can represent for the development of spintronic applications, it is very curious to notice that no other groups have reported on this phase. It is probable that the growth process window allowing stabilizing this phase can be extremely narrow [12, 18]. In addition, what may become complicated is that not all nanocolumns could exhibit a high Curie temperature [14]. Thus, one of the important starting points of our works consists in determining growth conditions, allowing to *reproducibly* synthetize this phase. For this reason and as mentioned in our previous studies [19, 20, 21], we have first investigated the GeMn growth in an intermidiate temperature range of 100-150 $^\circ$C and at each growth temperature a large a Mn concentration in the range from 4 to 8 % has been experienced. For each experiment, TEM and magnetic characterizations were systematically used to verify the structural and magnetic output of the layers. These preliminary investigations have allowed us to determine a growth temperature of 130 $^\circ$C to study the GeMn nanocolumn composition.

At the growth temperature of 130 $^\circ$C and Mn content of $\sim$6 %, Fig. 1 displays typical cross-sectional (a) and plan–view (b) TEM images of the sample. Dark contrast corresponds to Mn-rich regions while regions with a brighter contrast arise from the diluted matrix. The corresponding film thickness is $\sim$80 nm. According to an overall view of the layer structure, we can see that the GeMn nanocolumns observed here are orientated along the (001) direction and entirely coherent with the surrounding diluted matrix. The average diameter of these nanocolumnsh is $\sim$5 - 8 nm, which is slightly higher than those previously reported in [12].

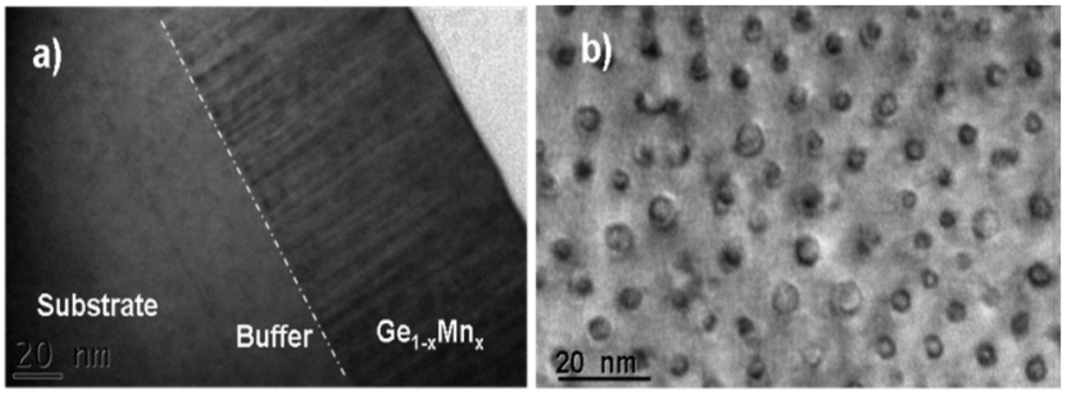

Fig. 1. Typical cross-sectional (a) and planeview (b) TEM images of a 80 nm thick Ge_1 $-$ xMn$_x$ film grown at 130 $^\circ$C and with $x \sim 0.06$.

Determination the chemical composition of nanocolumns represents a crucial step in order to correlate the above structural properties. In [12] and 15, the authors have used electron energy-loss spectroscopy (EELS) and deduced an average Mn concentration, ranging between 37.5% and 32% inside nanocolumns. The nanocolumn composition was supposed to be close to Ge_2Mn, an unknown germanium-rich phase. While the above experiments have been carefully undertaken

and EELS is known as a nano-scaled composition analysis tool, a precise determination of composition in nanocolumns using EELS could be affected by an overlap of Ge signals coming from the surrounding matrix.

LP-APT is a three-dimensional useful technique in analysis of subsurface or buried features in specimens with very high sensitivity. The high spatial resolution of the technique makes it especially practical in the investigation the size, the composition, the morphology, and the evolution of the solute segregation [21]. Taking these advantages of LP-APT for further confirming the structural properties of the sample, we respectively present in Fig. 2(a) and (b) LP-ATP cross-sectional and plan-view images of a sample with a Mn concentration of $\sim 6\%$.

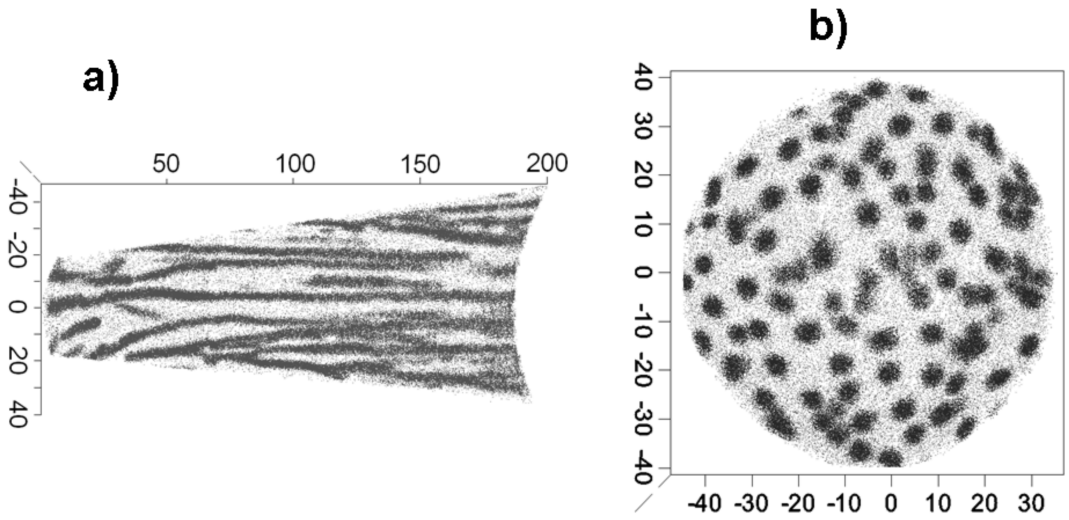

Fig. 2. a) LP-APT cross section view image of 100 nm-thick slab showing 1% of detected Ge atoms (red dots) and 100% of detected Mn atoms (purple dots). b) LP-APT plan view image of 20 nm-thick slab showing 3% of detected Ge atoms (red dots) and 100% of detected Mn atoms (purple dots). Scales are in nanometers.

Fig. 2(a) displays a cross-sectional image corresponding to a 10 nm-thick slab showing 1% of detected Ge atoms (red dots) and 100% of detected Mn atoms (purple dots). Scales indicated in the image are in nanometers. The image confirms the columnar structure observed along the growth direction of the sample. Nanocolumns are continuous but not straight, most of them are not crossing the entire layer of 200 nm-thick. The ATP plan-view image in Fig. 2(b) exhibits an excellent match with the plan-view TEM image show in Fig. 1(b), Mn atoms are found to be concentrated in regions of an average diameter of ~ 5 nm. It is worth noting that Mn atoms with a much lower concentration are also found in the matrix in-between nanocolumns.

A feature of particular interest of the LP-APT technique is that it can excel three-dimensional compositional distribution of elements in a volume. Fig. 3(a) represents three different views of a three-dimensional volume containing three nano-columns referenced as #1, #2 and #3, which have been randomly chosen. In this representation, a colored sphere is plotted at the position of each atom and only Mn atoms are shown. From these Mn atom maps, we can see that columns are free of Mn-rich precipitates and are richer in Mn in regions close to the surface.

To illustrate the interesting information concerning the Mn distribution in nanocolumns presented in Fig. 3(a) (#1, #2 and #3), Fig. 3(b) displays one-dimensional profile of Mn concentration through two adjacent columns in a plan that is perpendicular to the growth direction. The figure reveals three important pieces of information: first, the Mn concentration across a nanocolumn is not homogenous, nanocolumns exhibit a core-shell structure with a much higher Mn concentration in the core compared to that of the shell. The second information is that the Mn concentration in the matrix in-between nanocolumns is much less variable, an *average* value of $\sim$0.5% can be deduced. Third, at the same depth neighbors columns exhibit almost the same Mn concentration.

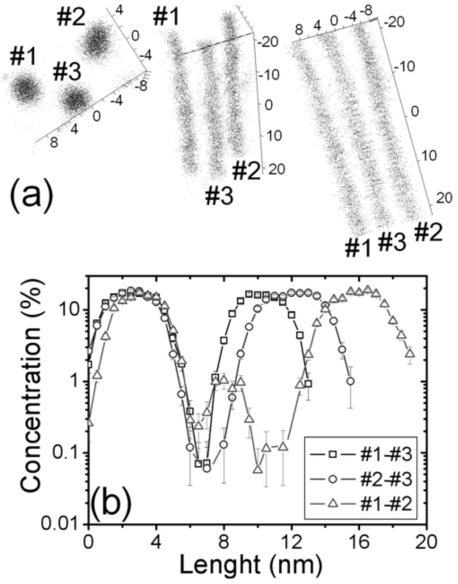

Fig. 3. a) Three different views of a three-dimensional volume containing three nano-columns referenced as #1, #2 and #3 (each dot is a single Mn atom). b) one-dimensional Mn concentration profiles through two columns: #1 and #3 (squares), #2 and #3 (circles), #1 and #2 (triangles).

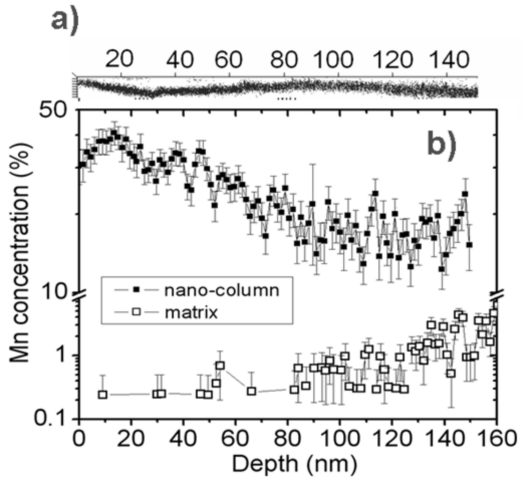

Fig. 4. a) Distribution of Mn atoms (purple dots) in a single nano-column. b) Mn concentration versus depth in the single nano-column presented in (a) (solid symbols) and in the matrix (open symbols).

By choosing a single nanocolumn and determine the profile of the Mn concentration along it at the atomic scale by mean of LP-APT, we are able to precisely determine the chemical composition of nanocolumns and of the surrounding matrix. As can be seen in Fig. 2(a), nanocolumns have different lengths and all of them are not nucleated from the interface with the Ge buffer layer. We have thus chosen one of the longest nanocolumns, which has a length of about 140 nm (Fig. 4(a)) and is nucleated at the interface. We display in Fig. 4(b) a one-dimensional depth profile of the Mn concentration along this nanocolumn and in Fig. 4(b), the depth profile of the matrix neighboring to this nanocolumn. It is interesting to notice that the Mn concentration along a nanocolumn is highly inhomogeneous, not only along the whole length but also between two adjacent points. Starting from the surface toward the interface, the Mn concentration along the nanocolumn is found to decrease from $\sim$ 40% down to $\sim$ 20%. The variation of the Mn concentration in the matrix is, in contrary, much less important except the regions near the interface

region. The lowest value is about 0.25 % and can reach a highest value of $\sim$1% in regions close to the interface. The above results clearly indicate that the Mn concentration along nanocolumns cannot be represented by an *average* value and thus *cannot* attributed to a *well-defined* compound. It is highly inhomogeneous and continuously increases from its bottom to the top on the surface.

IV. CONCLUSION

In conclusion, by using LP-APT analyses, we are able to provide the first *direct* measurement of the Mn concentration inside nanocolumns and in the diluted matrix at atomic scale. The Mn concentration inside nanocolumns is found to be highly inhomogeneous, it is about 20% at the bottom and can increase up to $\sim$40% in the top near the surface region. GeMn nanocolumns are found to exhibit a core-shell structure, the core has a diameter of $\sim$2 nm and has a higher Mn concentration. The variation of the Mn concentration in the matrix is about 0.25 % at the surface and can reach a highest value of $\sim$1% in regions close to the interface. Thus, the nanocolumns phase is not a compound having a well-defined composition but may be considered as a Ge-Mn solid solution with a variable composition. For better understanding the formation mechanism of high-T_C nanocolumns, it is necessary to carry on with more measurements for explanation. Working on this direction is in progress.

ACKNOWLEDGMENTS

This work was supported by the National Foundation for Science and Technology Development (NAFOSTED) under grant number of **103.02-2013.66.** The authors would like to thank Prof. Vinh LE THANH and Dr. Minh Tuan DAU - Centre Interdisciplinaire de Nanoscience de Marseille (CINaM-CNRS), France for their helps.

REFERENCES

[1] T. Dietl, H. Ohno, F. Matsukura, J. Cibert, and D. Ferrand, *Science* **287** (2000) 1019.
[2] Y. D. Park, A. T. Hanbicki, S. C. Erwin, C. S. Hellberg, J. M. Sullivan, J. E. Mattson, T. F. Ambrose, A. Wilson, G. Spanos, and B. T. Jonker, *Science* **295** (2002) 651.
[3] S. Cho, S. Choi, S.C. Hong, Y. Kim, J.B. Ketterson, B.-J. Kim, Y.C. Kim, J.-H. Jung, *Phys. Rev. B* **66,** (2002) 033303.
[4] A.P. Li, J. Shen, J.R. Thompson, H.H. Weitering, *Appl. Phys. Lett.* **86** 152507 (2005);
[5] Y. Shuto, M. Tanaka, and S. Sugahara, *J. Appl. Phys.* **99** (2006) 08D516.
[6] D. Bougeard, S. Ahlers, A. Trampert, N. Sircar, and G. Abstreiter, *Phys. Rev. Lett.* **97** (2006) 237202.
[7] S. Ahlers, D. Bougeard, N. Sircar, G. Abstreiter, A. Trampert, M. Opel, and R. Gross, *Phys. Rev. B* 74, (2006) 214411.
[8] E. Biegger, L. Stäheli, M. Fonin, U. Rüdiger, and Yu. S. Dedkov, *J. Appl. Phys.* **101** (2007) 103912.
[9] J.-S. Kang, G. Kim, S. C. Wi, S. S. Lee, S. Choi, S. Cho, S. W. Han, K. H. Kim, H. J. Song, H. J. Shin, A. Sekiyama, S. Kasai, S. Suga, and B. I. Min, *Phys. Rev. Lett.* **94** (2005) 147202.
[10] Y.D. Park, A. Wilson, A.T. Hanbicki, J.E. Matteson, T. Ambrose, G. Spanos, B.T. Jonker, *Appl. Phys. Lett.* **78**, (2001) 2739.
[11] C. Zeng, S. C. Erwin, L. C. Feldman, A. P. Li, R. Jin, Y. Song, J. R. Thompson, and H. H. Weitering, *Appl. Phys. Lett.* **83** (2003) 5002.
[12] M. Jamet, A. Barski, T. Devillers, V. Poydenot, R. Dujardin, P. Bayle-Guillemaud, J. Rothman, E. Bellet-Amalric, A. Marty, J. Cibert, R. Mat-tana, and S. Tatarenko, *Nat. Mater.* **5** (2006) 653.
[13] D. Bougeard, S. Ahlers, A. Trampert, N. Sircar, and G. Abstreiter, *Phys. Rev. Lett.* **97**, (2006) 237202.
[14] D. Bougeard, N. Sircar, S. Ahlers, V. Lang, G. Abstreiter, A. Trampert, J. M. LeBeau, S. Stemmer, D. W. Saxey, and A. Cerezo, *Nano Letters* **9** (2009) 3743.

[15] T. Devillers, M. Jamet, A. Barski, V. Poydenot, P. Bayle-Guillemaud, E. Bellet-Amalric, S. Cherifi, J. Cibert, *Phys. Rev. B* **76** (2007) 205306.
[16] L. Ottaviano, M. Passacantando, S. Picozzi, A. Continenza, R. Gunnella, A. Verna, G. Impellizzeri, F. Priolo, *Appl. Phys. Lett.* **88** (2006) 061907.
[17] C. Bihler, C. Jaeger, T. Vallaitis, M. Gjukic, M.S. Brandt, E. Pippel, J. Woltersdorf, U. Gosele, *Appl. Phys. Lett.* **88** (2006) 112506.
[18] T-G. Le , M-T. Dau, V. Le thanh, D. N. H. NAM, M. Petit, L.A. Michez, N.V. Khiem and M.A. NGUYEN, *Adv. Nat. Sci.: Nanosci. Nanotechnol.* **3**, (2012) 025007.
[19] T-G. Le, D. N. H Nam, M-T. Dau, T. K. P Luong, N. V. Khiem, V. Le Thanh, L.A. Michez and J. Derrien, *Journal of Physics: Conference Series* **292** (2011) 012012.
[20] T. B. Massalki, Binary alloy phase diagrams, 2nd Edition, Vol 1, 2, ASM International 1992.
[21] Thomas F. Kelly and Michael K. Miller, Invited Review Article: Atom probe tomography, *Review of Scientific Instruments* **78** (2007) 031101.